EUKARYOTIC CELL, Feb. 2008, p. 319–327 Vol. 7, No. 2
1535-9778/08/$08.00+0 doi:10.1128/EC.00378-07

Cryptococcus neoformans Capsular Polysaccharide and Exopolysaccharide Fractions Manifest Physical, Chemical, and Antigenic Differences▽

Susana Frases,[1] Leonardo Nimrichter,[2] Nathan B. Viana,[3,4] Antonio Nakouzi,[1] and Arturo Casadevall[1,5]*

Department of Microbiology and Immunology[1] and Division of Infectious Diseases of the Department of Medicine,[5] Albert Einstein College of Medicine, Bronx, New York 10461, and Laboratório de Estudos Integrados em Bioquímica Microbiana, Instituto de Microbiologia Paulo de Góes,[2] LPO-COPEA, Instituto de Ciências Biomédicas,[3] and Instituto de Física,[4] Universidade Federal do Rio de Janeiro, Rio de Janeiro 21941-590, Brazil

Received 14 October 2007/Accepted 16 December 2007

The human pathogenic fungus *Cryptococcus neoformans* has a large polysaccharide (PS) capsule and releases copious amounts of PS into cultures and infected tissues. The capsular PS is a major virulence factor that can elicit protective antibody responses. PS recovered from culture supernatants has historically provided an ample and convenient source of material for structural and immunological studies. Two major assumptions in such studies are that the structural features of the exopolysaccharide material faithfully mirror those of capsular PS and that the isolation methods do not change PS properties. However, a comparison of exopolysaccharide made by two isolation techniques with capsular PS stripped from cells with gamma radiation or dimethyl sulfoxide revealed significant differences in glycosyl composition, mass, size, charge, viscosity, circular-dichroism spectra, and reactivity with monoclonal antibodies. Our results strongly suggest that exopolysaccharides and capsular PS are structurally different. A noteworthy finding was that PS made by cetyltrimethylammonium bromide precipitation had a larger mass and a different conformation than PS isolated by concentration and filtration, suggesting that the method most commonly used to purify glucuronoxylomannan alters the PS. Hence, the method used to isolate PS can significantly influence the structural and antigenic properties of the product. Our findings have important implications for current views of the relationship between capsular PS and exopolysaccharides, for the generation of PS preparations suitable for immunological studies, and for the formulation of PS-based vaccines for the prevention of cryptococcosis.

Cryptococcus neoformans is an encapsulated fungus that is the causative agent of cryptococcosis, a life-threatening disease, particularly in situations of compromised immunity. The cryptococcal capsule is a complex structure that is considered the key virulence factor for this pathogen (8). The capsule is composed of two major polysaccharides (PSs), galactoxylomannan (GalXM) and glucuronoxylomannan (GXM). GalXM is an α-(1,6) galactan with branches of β(1,3)-galactose-α(1,4)-mannose-α(1,3)-mannose. Xylose units can be associated to branched mannose through β(1,3) or β(1,2) linkages (22). GalXM has an average mass of 100 kDa and has potent deleterious effects on immunological function (11, 12, 18). GXM is a high-molecular-mass PS with a complex structure. The weight-averaged mass (M_w) is 1,700 to 7,000 kDa (12), which makes up about 90% of the capsule mass. Structurally, GXM consists of a linear α-(1,3)-mannan main chain with β(1,2)-glucuronic acid residues attached to every third mannose, on average. Mannosyl residues can also be 6-*O* acetylated and substituted with xylosyl units in β(1,2) or β(1,4) linkages (11). GXM and GalXM are released into culture medium by growing cells as exopolysaccharides that can be recovered in sufficient quantities for physical and chemical analysis.

Although the biological and structural properties of GXM have been extensively studied, its physical properties remain relatively unexplored. Given that GXM is a macromolecule and that capsular assembly involves the noncovalent attachment of PS fibrils to the cell wall (6, 19), it is likely that many properties of the capsule are directly related to physicochemical properties of the PS molecules. For example, there is evidence that capsular assembly is at least partly the result of inherent PS properties that promote self-assembly (12). GXM is believed to contribute to virulence by interfering with the host immune response by multiple mechanisms (13) that are almost certainly related to intrinsic PS structural properties. Some antibodies to GXM are protective, and this PS can provide important components for a vaccine against cryptococcosis (5). Despite the extensive studies carried out with GXM, it is noteworthy that practically all of our information about *C. neoformans* capsular PS originates from studies of exopolysaccharide components released from cells and recovered from culture supernatants. However, a correspondence of identity between the structures of capsular PS and exopolysaccharide has been assumed without experimental verification.

In the present study, we report that different methods of purifying extracellular PS from strain 24067 of *C. neoformans* grown under the same conditions yield PS preparations with

* Corresponding author. Mailing address: Department of Microbiology and Immunology, Albert Einstein College of Medicine, 1300 Morris Park Avenue, Bronx, NY 10461. Phone: (718) 430-2215. Fax: (718) 430-8968. E-mail: casadeva@aecom.yu.edu.
▽ Published ahead of print on 21 December 2007.

different physical, chemical, and serological properties. Comparison of soluble PS with PS directly released from the surface of *C. neoformans* by gamma radiation or dimethyl sulfoxide (DMSO) treatment revealed significant differences from exopolysaccharide material. The characterization of the physical chemical properties of cell-associated and extracellular PS provides new insight into the relationship between exopolysaccharides and capsular PS.

MATERIALS AND METHODS

***C. neoformans* cultures.** *C. neoformans* strain ATCC 24067 was grown in a minimal medium composed of glucose (15 mM), $MgSO_4$ (10 mM), KH_2PO_4 (29.4 mM), glycine (13 mM), and thiamine-HCl (3 μM), pH 5.5. Fungal cells were cultivated for 7 days at 30°C.

Isolation of PS from culture supernatants by cetyltrimethylammonium bromide precipitation (CTAB-PS). Extracellular PS (exopolysaccharide) was isolated as described by Cherniak et al. (4), with the minor modifications proposed by Mc Fadden et al. (12). Briefly, supernatants were obtained by centrifugation of fungal cultures and filtered through 0.45-μm-pore-size filters to remove remaining yeast cells and cell debris. The PS was then isolated from supernatants by addition of sodium acetate (10% [wt/vol], final concentration), and the solution pH was immediately adjusted to 7.0 with acetic acid to avoid destruction of acetyl groups. Then, 2.5 volumes of 100% ethanol was added to precipitate the PS. The PS precipitate was separated from the supernatant by centrifugation, and the pellet was then dissolved in water. The carbohydrate content was determined by the phenol sulfuric acid method (12). The PS solution was then adjusted with NaCl (0.2 M, final concentration), and PS was selectively precipitated by adding 3 g of CTAB (Sigma, St. Louis, MO) per g of carbohydrate. The CTAB-PS complex, recovered by centrifugation, was then dissolved in 1 M NaCl and precipitated again by the addition of 2.5 volumes of 95% ethanol. In this step, the addition of ethanol will precipitate the PS while most of the CTAB remains in the NaCl solution. After centrifugation, the supernatant was discarded and the PS was dissolved in 2 M NaCl, dialyzed extensively against 1 M NaCl to remove the CTAB, and then dialyzed against distilled water for 2 days. The PS solution was then lyophilized, and the mass was determined in an analytical balance. Samples obtained by CTAB precipitation are referred to as CTAB-PS. The effects of CTAB on PS were also evaluated by addition of 0.1% CTAB solution to a 1-mg/ml solution of F-PS, GR-PS, and DMSO-PS. These samples will be referred to CTAB-F-PS, CTAB-GR-PS, and CTAB-DMSO-PS.

Isolation of PS from culture supernatants by filtration. Based on the ability of PS to self-aggregate, the PS was isolated by filtration and ultrafiltration as described recently (17). Briefly, *C. neoformans* cells were separated from culture supernatants by centrifugation and the resulting supernatant was concentrated approximately 20-fold with an Amicon (Millipore, Danvers, MA) ultrafiltration cell (cutoff of 100 kDa, total capacity of 200 ml) with stirring and Biomax polyethersulfone ultrafiltration discs (76 mm; Millipore, Danvers, MA). After formation of a viscous film over the filtering disc, the fluid phase was discarded and the remaining jellified material was recovered with a cell scraper. The final PS solution was lyophilized, and the dry PS mass was determined. Samples obtained by filtration were named F-PS.

Release of capsular components by gamma radiation. Capsular PS was isolated as described by Maxson et al. (10). Yeast cells were washed three times in Milli-Q water to remove shed capsular PS and suspended in fresh water. The cells were then radiated with a Shepherd Mark I irradiator (JL Shepherd and Associates, San Fernando, CA) at a dose rate of 1,388 rads/min for 60 min. Irradiated cells were removed by centrifugation, and the soluble phase was collected for lyophilization. PS fractions obtained from the cell surface of *C. neoformans* by irradiation were named capsular GR-PS. The effects of gamma radiation on cell-free PS solutions were also evaluated by irradiating PS fractions under the conditions described above. These samples were named R-CTAB-PS and R-F-PS.

Release of capsular components by DMSO. Capsular PS was isolated as described by Bryan et al. (2). Yeast cells were washed three times in Milli-Q water. The cells were suspended in 15 ml of DMSO and incubated for 30 min twice. Cells were removed by centrifugation, and the supernatant was then dialyzed against water for 12 h, with water replacement with fresh water at 2-h intervals, and then extensively dialyzed against water for 3 days. PS fractions obtained from the cell surface of *C. neoformans* by DMSO were named capsular DMSO-PS. The effects of DMSO on PS were also evaluated by addition of DMSO to CTAB-PS, F-PS, and GR-PS. These samples are referred to as DMSO-CTAB-PS, DMSO-F-PS, and DMSO-GR-PS.

Effect of GalXM on PS. F- and R-F-PS solution was mixed with purified GalXM at a ratio 80:20 (wt/wt). Physical parameters were measured as described below.

Glycosyl composition of PS-containing fractions. PS fractions were dissolved in methanol–1 M HCl and incubated at 80°C for 18 h. Methanolyzed samples were then per-*O*-trimethylsilylated by treatment with Tri-Sil (Pierce) for 30 min at 80°C. The per-*O*-trimethylsilylated derivatives were analyzed by gas chromatography (GC) coupled to mass spectrometry. The derivatized structures were first separated on an HP 5890 gas chromatograph with a Supelco DB-1 fused silica capillary column (30 m by 0.25 mm [inside diameter]). Peaks detected by GC were fragmented in a 5970 MSD mass spectrometer interfaced with the gas chromatograph. Carbohydrate standards included arabinose, rhamnose, fucose, xylose, glucuronic acid, galacturonic acid, mannose, galactose, glucose, mannitol, dulcitol, and sorbitol. The average and standard deviation of three different extractions were calculated.

Nuclear magnetic resonance (NMR) spectroscopy of capsular PS. The sample was partially depolymerized by probe sonication for 30 min at 0°C and de-*O*-acetylated by adjusting the solution to pH 11 with concentrated ammonium hydroxide, followed by incubation at 25°C for 20 h. After lyophilization, the sample was deuterium exchanged by lyophilization from D_2O (99.9% D), dissolved in 0.28 ml D_2O (99.96% D), filtered (0.45 μm), and transferred to an NMR tube with susceptibility plugs (Shigemi Inc., Allison Park, PA). A 1D proton NMR spectrum was acquired on a Varian Inova 600-MHz spectrometer at 343 K (70°C). The spectral width was 3,605 Hz, the acquisition time was 2.05 s, and 256 scans were collected. The spectrum was processed with the Mestre-C NMR software. Linear prediction to 16K and a Gaussian function (2-Hz line broadening) were applied to the flame ionization detector to obtain a full spectrum. Linear prediction to 16K, a 0.65°-shifted sinebell function, and a Gaussian function (2-Hz line broadening) were applied to obtain an enhanced-resolution partial spectrum of the region displaying the mannose anomeric protons. Chemical shifts were measured relative to internal 2,2-dimethyl-2-silapentane-5-sulfonic acid ($\delta = 0.00$ ppm). Spectra were analyzed to identify the structural reported groups described by Cherniak et al. (4).

Molecular mass determination. Molecular masses were calculated by multiangle laser light scattering as described by McFadden et al. (12). PS solutions were prepared with sterile-filtered, degassed, ultrapure water. All samples were passed through an in-line 0.8-μm syringe filter to eliminate large aggregates and reduce extraneous sources of refracted or scattered light. Differential refractometry with a 620-nm laser source (BI-DNDC; Brookhaven Instruments Corp., Holtsville, NY) was used to measure alterations in the refractive index (dn/dc) of the PS samples. Molecular masses were determined at 25°C by multiangle laser light scattering in a molecular weight analyzer (BI-MwA; Brookhaven Instruments Corp., Holtsville, NY) with a 675-nm laser source. Toluene was used for system calibration, and 20-nm microspheres were used for normalization of Rayleigh scattering (Duke Scientific Corp., Palo Alto, CA). The M_w was finally calculated by the Zimm equation, $Kc/\Delta R(\theta) = 1/(M_w)[P(\theta)] + 2A_2c$, where K is the optical constant, defined as the quotient $4\pi^2 n_o^2 (dn/dc)^2)/N_A\lambda^4_o$, and $\Delta R(\theta)$ is the excess Rayleigh factor, determined by comparing the sample and solvent values at angle θ and concentration c. $P(\theta)$ represents the particle-scattering function, A_2 is the second virial coefficient, n_o is the refractive index of the solvent, N_A equals Avogadro's number, and λ_o is the modal wavelength of the laser source. The dn/dc values were adjusted according to the Cauchy equation ($dn/dc = A + B/\lambda^2$) by using a B coefficient for aqueous solutions of +0.0022 μm and wavelengths (λ) in micrometers to accommodate for the longer wavelength of the molecular weight analyzer. Depolarization corrections were assumed to be negligible.

Zeta potential measurements. The zeta potential (ζ), particle mobility, and shift frequency of PS samples were calculated in a zeta potential analyzer (Zeta-Plus; Brookhaven Instruments Corp., Holtsville, NY). ζ is a measurement of charge (in millivolts) defined as the potential gradient that develops across the interface between a boundary liquid in contact with a solid and the mobile diffuse layer in the body of the liquid. It is derived from the equation $\zeta = (4\pi\eta m)/D$, where D is the dielectric constant of the medium, η is the viscosity, and m is the electrophoretic mobility of the particle.

Viscosity determinations. Brownian motion of polystyrene spheres (radius, 1.52 ± 0.05 μm) immersed in GXM solutions was used to determine viscosity. A suspension of spheres (1 μl, 10% [vol/vol]; Sigma, St. Louis, MO) was diluted in 150 μl of dialyzed GXM (1 mg/ml) to a final concentration of 10^{-4}% (vol/vol), transferred to a coverslip with an O ring 1 cm in diameter and 0.3 cm in width, and then sealed with a second coverslip. Samples were examined with an inverted Nikon Eclipse TE300 microscope connected by its epifluorescence port to an

TABLE 1. Glycosyl composition analysis of PS fractions

Sugar(s)	CTAB-PS[a]	F-PS[a]	GR-PS[a]	DMSO-PS[a]
Xyl	10.90 ± 0.62	13.97 ± 5.37	8.60 ± 4.61	5.70 ± 1.15
GlcA	9.87 ± 2.08	10.30 ± 2.68	7.90 ± 1.06	3.57 ± 0.25
Man	70.87 ± 4.01	74.03 ± 4.60	41.77 ± 2.31	21.00 ± 0.62
Gal	0.80 ± 0.26	1.23 ± 0.25	0.37 ± 0.32	0.53 ± 0.15
Glu	7.57 ± 1.57	0.40 ± 0.36	41.33 ± 1.10	69.2 ± 1.91
GlcA-Xyl-Man[b]	1:1.10:70.87	1:1.35:7.18	1:1.09:5.29	1:1.60:5.88

[a] Each values is the average mole percentage of each sugar. Errors are given as standard deviations of independent measurements.
[b] Ratio is normalized to GlcA.

Nd-YAG laser beam source (1,064-nm wavelength). When the laser beam passes through the objective, it creates an optical trap near the objective focus, allowing the manipulation of small dielectric objects (~μm length). The samples were observed with a Plan Apo 100× NA1.4 objective. Digitized images were obtained by a charge-coupled device camera connected to a Hamamatsu Argus and a Scion frame grabber. Images were processed with the ImageJ software (NIH, http://rsb.info.nih.gov/ij/). After positioning the bead at the desired height, h (the distance of the polystyrene sphere center to the glass coverslip), a small image area (50 by 50 pixels) was chosen for a frame capture rate of 27 to 28 frames/s. The optical tweezers were then alternately turned on and off for periods of circa 0.5 s by shutting the beam off.

The mean square displacement of the variation of the image center of mass position δρ in a time interval t is given by the equation

$$<(\delta\rho)^2> = 4Dt \quad (1)$$

where

$$D = \frac{k_B T}{\beta} \quad (2)$$

and β, the Stokes friction coefficient, is a function of the bead radius, a, and height, h. The height, h, was defined as the distance from the sphere center to the coverslip. β is given by the Faxen law as follows:

$$\beta = 6\pi\eta a\left[1 - \frac{9}{16}\left(\frac{a}{h}\right) + \frac{1}{8}\left(\frac{a}{h}\right)^3 - \frac{45}{256}\left(\frac{a}{h}\right)^4 - \frac{1}{16}\left(\frac{a}{h}\right)^5\right]^{-1} \quad (3)$$

For a fixed value of h, $<(\delta\rho)^2>$ was calculated by excluding the regions where δρ is <0.01 μm. Those regions correspond to the time intervals for which the bead was trapped. From the linear fit of the measured $<(\delta\rho)^2>$ values as a function of time, t, in equation 1, the diffusion coefficient, D, was obtained. With the value of D, the Stokes friction coefficient, β, was determined by using equation 2. The sphere height was then changed, and the procedure was repeated. From the fit of the β values as a function of sphere height, h, by using equation 3, viscosity values were obtained. The method described had 0 to 20% uncertainty in viscosity determinations.

Circular-dichroism (CD) analysis of PS fractions. CD measurements of the different PS samples were carried out on a Jasco J-720 spectropolarimeter (Jasco Inc., Easton, MD) with a 2-mm cell at 25°C. In all cases, samples contained 3 mM PS dissolved in ultrapurified water. The CD spectra were recorded in the wavelength region of 185 to 250 nm and were expressed as molar ellipticity ([θ]), which is corrected for concentration units in deg cm^2/dmol.

Binding of monoclonal antibodies (MAbs) to PS in polystyrene plates. Binding of MAbs to the different PS fractions was evaluated by enzyme-linked immunosorbent assay (ELISA) (3). Briefly, polystyrene plates were coated with 1 nM PS samples (with molecular masses determined in this study). The plates were blocked with phosphate-buffered saline (PBS) containing 1% bovine serum albumin. Anti-PS MAbs 18B7 (immunoglobulin G1 [IgG1]), 2D10 (IgM), 12A1 (IgM), and 21D2 (IgM) were then added to the plates, followed by detection of antibody binding to PS with alkaline phosphatase-labeled secondary antibodies. The MAbs bind to different epitopes in PS. Colored reactions were developed after the addition of *p*-nitrophenyl phosphate (*p*-NPP) solutions (Sigma, St. Louis, MO), and quantitative determinations were performed by absorbance measurement at 405 nm. All incubations were carried out at 37°C for 1 h.

Binding of MAbs to PS by dot blot analysis. PS samples (1 nM) were placed on nitrocellulose membranes. The membranes were dried for 1 h at 37°C and then blocked with PBS containing 1% bovine serum albumin. Membranes were incubated with the antibodies described above at 10 μg/ml. After extensive washing, the membranes were incubated with alkaline phosphatase-conjugated antibodies and *p*-NPP solutions. Reactions were quantified by transfer of the soluble colored products to 96-well plates and reading at 405 nm.

Binding of MAbs to PS by capture ELISA. Microtiter plates were coated with 50 μl of unlabeled anti-IgM antibody at a concentration of 1 μg/ml in PBS and incubated for 1 h at 37°C. Afterward, the plates were washed and the antibodies described above was added at 1 μg/ml. The plates were then incubated for 1 h at 37°C. The plates than were washed, and 1 nM PS was added. After 1 h of incubation at 37°C, MAb 18B7 was added to the wells at 1 μg/ml. After extensive washing, plates were incubated with alkaline phosphatase-conjugated antibodies and *p*-NPP solutions. Reactions were quantified at 405 nm.

Statistical analysis. Statistical analyses were carried out with Bi-ZPMwA Zimm Plot Software (Brookhaven Instruments Corp., Holtsville, NY) for M_w, Rg, and A_2. 90Plus/BI-MAS software was used for comparison of effective-diameter, polydispersity, and diffusion coefficient values (Brookhaven Instruments Corp., Holtsville, NY). Zeta Plus software was used for comparisons of zeta potential, mobility, and frequency shift data (Brookhaven Instruments Corp., Holtsville, NY).

RESULTS

Glycosyl composition analysis. PS samples were subjected to acidic methanolysis, and their monosaccharide constituents were analyzed by GC. This analysis allows the potential detection of four different forms of each sugar derivative, corresponding to the α and β forms of furanose and pyranose rings. In association with mass spectrometry analysis, each peak can be identified precisely on the basis of the fragmentation profile observed. Fragmentation of per-*O*-trimethylsilylated derivatives of hexoses usually generates diagnostic peaks at m/z 217 and 214. The (m/z 204)/(m/z 217) ratio of pyranose rings is >1, whereas that of furanose rings is <1. Peaks with retention times corresponding to standard derivatives of the typical cryptococcal PS components mannose (Man), xylose (Xyl), and glucuronic acid (GlcA) were detected in the hydrolysates (Table 1). For CTAB and F-PS, Man was the major monosaccharide constituent, followed by Xyl and GlcA. Different proportions of monosaccharide constituents were observed in GR-PS and DMSO-PS, which presented, respectively, Man-Xyl-GlcA average molar ratios of 41.77:8.60:7.90 and 21.00:5.70:3.57, respectively. Galactose and glucose were the only sugars other

TABLE 2. dn/dc, M_w, Rg, M_w/Rg, A_2, and rigidity for five and three sugars of PS fractions calculated by multiangle laser light scattering in a molecular weight analyzer

PS sample	dn/dc (620 nm)	M_w (10^6 g/mol)[a]	Rg (nm)[a]	M_w/Rg (10^3)	A_2 (10^3 cm^{3}mol/g^2)[a]	Rigidity	
						5 sugars	3 sugars
CTAB-PS	0.1032	1.21 ± 0.12	55.8 ± 9.5	21.68	−11 ± 1.9	0.4180	0.6967
F-PS	0.1474	0.30 ± 0.05	159 ± 19	1.89	10 ± 4.3	13.5541	22.5900
GR-PS	0.1948	0.27 ± 0.05	151 ± 18	1.79	1.14 ± 1.8	12.3467	20.5777
DMSO-PS	0.1877	199 ± 0.62	255 ± 45	780.39	2.15 ± 1.5	0.0531	0.0885

[a] Values are averages and standard deviations.

TABLE 3. Charge, mobility, and frequency shift values of PS fractions calculated by Zeta potential analyzer[a]

PS sample	Zeta potential (mV)	Mobility [(μm/s)/(V/cm)]	Frequency shift (Hz)
CTAB-PS	−41.66 ± 0.68	−3.25 ± 0.05	−24.22 ± 0.37
F-PS	−36.03 ± 1.04	−2.82 ± 0.08	−17.45 ± 0.52
GR-PS	−31.85 ± 1.85	−2.49 ± 0.11	−15.64 ± 0.67
DMSO-PS	−45.56 ± 2.95	−3.56 ± 0.23	−25.95 ± 1.91

[a] Values are averages and standard deviations.

than Man, GlcA, and Xyl detected in the samples. The average molar ratio of Gal was 0.80% for CTAB-PS, 1.23% for F-PS, 0.37% for the GR-PS, and 0.53% for the DMSO-PS. The presence of galactose probably denotes the presence of GalXM, another exocellular capsular PS of *C. neoformans*. A large amount of glucose was measured in GR-PS and DMSO-PS, which may reflect release of glucans from the *C. neoformans* cell wall since glucans make up >80% of the cell wall PSs (9). To investigate the origin of the glucose, the acapsular mutant Cap67 cells were extracted with DMSO. The results showed an average molar ratio of 4.6:32.6:4.3:21.1:37.4 for Xyl, Man, Gal, Glu, and *N*-acetylglucosamine, respectively, a finding suggesting a cell wall or cell body origin for the glucose found in DMSO-PS. DMSO-PS also contained fatty acids that are presumably solubilized by the organic solvent.

NMR spectroscopy of capsular PS. Based on previous reports on the structure of extracellular GXM from strain ATCC 24067 (1, 4), structural reporter groups and branches have been identified confirming that the currently characterized molecule represents serotype D PS motif 1. Given the glycosyl heterogeneity of the PS fractions, we studied the DMSO-PS (capsular PS) by NMR spectroscopy to relate our results to prior studies. In previous studies, the CTAB-PS fraction of strain 24067 was shown to be overwhelmingly composed of structural motif 1. However, we recently described a new reporter group in the F-PS fraction of this strain (17). NMR analysis of DMSO-PS revealed the expected motif 1 GXM spectrum (data not shown).

Average molecular mass, radius of gyration, and second virial coefficients of PS. Multiangle laser light scattering was used to determine the average molecular mass (M_w) of PS from the different preparations. The masses of the different PS preparations were derived from Zimm plots of light-scattering data (Table 2). The largest mass of PS was that of the DMSO-PS, followed by CTAB-PS, F-PS, and GR-PS. The radius of gyration (*Rg*) and the second virial coefficient (A_2) were also calculated from the light-scattering data (Table 2). The *Rg* is the average distance from the center point of the PS to the outer edge of the molecule. The *Rg* measurements of the different PS samples manifested substantial differences. The *Rg* was used in conjunction with the M_w to calculate the mass density of each PS sample. This analysis revealed that the DMSO-PS was 412-fold denser than the PS obtained by filtration or released by gamma radiation. PS-CTAB was approximately 12-fold denser than F- and GR-PS. Overall, the results showed that F-PS and GR-PS were more similar to each other than to DMSO- and CTAB-PS, with the caveat that each preparation manifested significant differences in one or more of the variables studied.

The rigidity of PS preparations was calculated as described by Sist et al. (21) from the M_w and *Rg* data. The equation Rg^2/Nw, where *Nw* is the average mass of sugar residues in the PS, was applied to the data for each sample. Rigidity was calculated on the basis of the five sugar residues (three Man, one GlcA, and one Xyl) in motif 1 (M1) of the serotype D PS described by Cherniak et al. and confirmed in this study by NMR (4) corresponding to that of strain 24067 and based on only the three mannoses in the backbone (Table 2). Considering only the mannose backbone, the pattern of rigidity followed that calculated for the complete motif.

Zeta potential, mobility, and frequency shift. Zeta potential determinations of PS preparations (Table 3) revealed that the

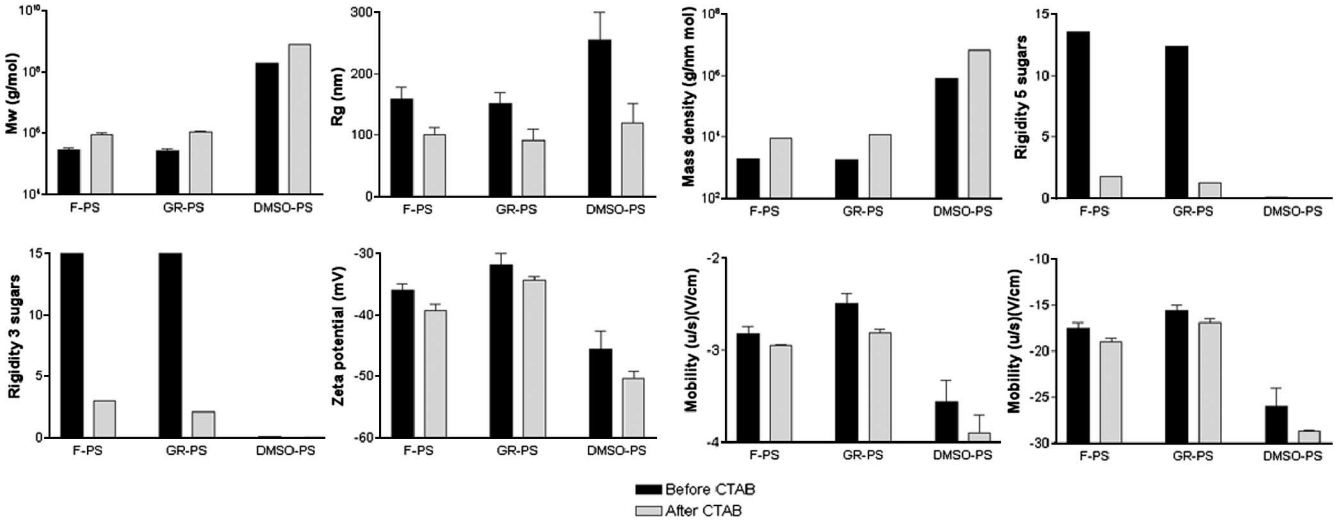

FIG. 1. Effects of CTAB on physical and chemical parameters. Black bars represent PS fraction before CTAB addition. Gray bars represents PS fractions after CTAB addition.

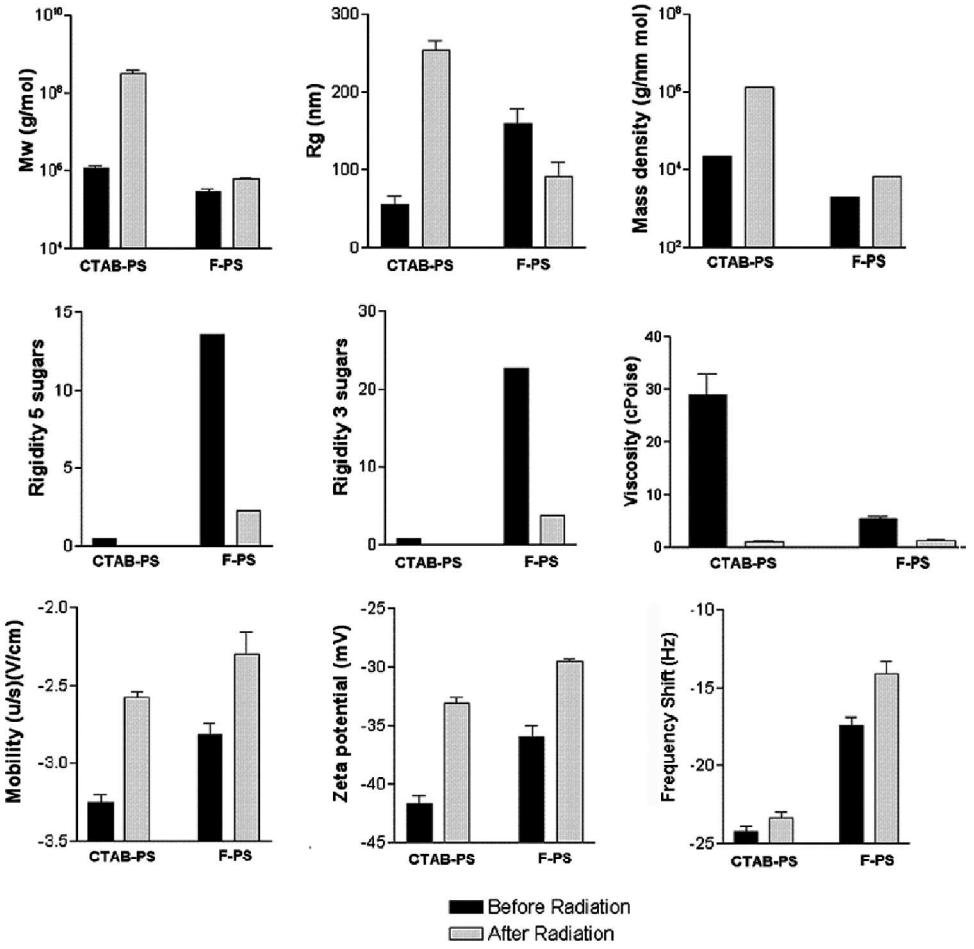

FIG. 2. Effects of gamma radiation on physical and chemical parameters. Black bars represent PS fraction before radiation treatment. Gray bars represents PS fractions after radiation treatment.

most negative values were obtained for DMSO-PS, followed by CTAB-PS, F-PS, and GR-PS. The negativity of mobility values and frequency shift of each sample followed the same pattern (Table 3).

Effect of CTAB on PS. To evaluate the effect of CTAB on the PS, F-PS, GR-PS, and DMSO-PS, these preparations were incubated with a solution of 0.1% CTAB and the various physical parameters were determined. After treatment with CTAB, the M_w of F-PS increased from 3×10^5 g/mol to 9×10^5 g/mol and the *Rg* was reduced by 1.6-fold, a phenomenon that may reflect aggregation or cross-linking of PS molecules (Fig. 1). For GR-PS, addition of CTAB resulted in the M_w increasing from 2.7×10^5 to 1.1×10^6g/mol while the value of *Rg* decreased approximately 61% (Fig. 1). For DMSO-PS, addition of CTAB resulted in an apparent increase in M_w from 1.99×10^8 to 8×10^8g/mol, with the value of *Rg* decreasing approximately 47%. Values of zeta potential, mobility, and frequency shift for each preparation were more negative after addition of CTAB (Fig. 1).

Effect of gamma radiation on PS. Taking into consideration that some of the differences measured for GR-PS relative to the other PS fractions reflected radiation effects on PS, the CTAB- and F-PS preparations were irradiated for 60 min and the physical parameters described above were determined. The M_w of CTAB-PS increased from 1.2×10^6 g/mol to 3.2×10^8 g/mol after gamma irradiation, possibly by cross-linking molecules. Values for zeta potential, mobility, and frequency shift were less negative for both samples after radiation (Fig. 2).

Effect of DMSO on PS. To evaluate the effect of DMSO molecules on the PS, CTAB-PS, F-PS, and GR-PS were incubated with DMSO as described before and all of the physical parameters described above were determined and no significant differences were observed (Table 4).

Effect of GalXM on PS. To study the effect of GalXM on the PS, we added GalXM solution to F-PS and R-F-PS. The results showed that addition of GalXM to F-PS and R-F-PS modified the physical properties of the PS, showing aggregation of PS fibers (Tables 5 and 6).

CD of PS. The secondary structure of PS was studied by CD spectroscopy (Fig. 3). The CD spectrum was devoid of large bands, except for the far-UV region, consistent with the absence of chromophores in PS. Interestingly, CTAB-PS demonstrated a large molar ellipticity band centered at 187 nm (Fig. 3A). Comparison of the CD spectra of irradiated and nonirradiated PS revealed radiation-induced changes consistent with secondary-structure changes (Fig. 3B). The effect in the

TABLE 4. Effect of DMSO treatment on M_w, *Rg*, rigidity, zeta potential, mobility, and frequency shift of PS samples

PS sample treated with DMSO	M_w (10^6 g/mol)[a]	*Rg* (nm)[a]	Rigidity		Zeta potential (mV)[a]	Mobility [(μm/s)/(V/cm)][a]	Frequency shift (Hz)[a]
			5 sugars	3 sugars			
CTAB-PS	2.0 ± 0.2	56.5 ± 2.12	0.259	0.432	−40.34 ± 0.40	−3.20 ± 0.01	−24.11 ± 0.35
F-PS	0.31 ± 0.07	158.2 ± 23.1	13.115	21.858	−35.47 ± 0.04	−2.78 ± 0.18	−17.30 ± 0.12
GR-PS	0.25 ± 0.01	150.2 ± 2.12	14.600	24.335	−30.32 ± 0.23	−2.38 ± 0.31	−17.10 ± 0.10

[a] Values are averages and standard deviations.

CD spectra with CTAB and non-CTAB PS treatment revealed conformational changes (Fig. 3C).

Reactivity with MAbs. We evaluated the epitope contents of the various PS fractions by reactivity with four MAbs that bind different epitopes. Three different assays were used, i.e., ELISA with polystyrene-adsorbed PS, dot blot analysis with membrane-immobilized PS, and capture ELISA. The rationale for employing different serological assays is that antibody reactivity for PS varies with the method used (7). Irrespective of the method used, we noted significant differences in the binding of MAb to PS fractions isolated by the various methods (Fig. 4).

DISCUSSION

Given the importance of the capsular PS in the pathogenesis of cryptococcal infections, it is not surprising that it has been the subject of extensive studies. However, practically all structural and immunological studies have utilized the soluble PS (exopolysaccharide) that accumulates in culture supernatants during in vitro growth, since this material is available in milligram quantities and is easily amenable to purification. However, the conclusions of many studies have been predicated on two assumptions that have not been validated experimentally. Firstly, it is generally thought that exopolysaccharide is derived from capsular PS and, consequently, that this material mirrors capsular PS with respect to structure and biological properties. However, our results showing major differences in the physical and chemical properties of PS isolated from supernatant and capsule raise significant questions about the validity of this assumption. Secondly, it has been assumed that the methodology of purification delivers a PS product in its native state. Strong evidence against the second assumption was provided by a recent study showing that exopolysaccharide isolated by concentrating and filtering culture supernatants was significantly smaller than CTAB-purified PS from *C. neoformans* (17). Consequently, we have systematically analyzed the physical, chemical, and antigenic properties of PS prepared by four different techniques and isolated from the supernatants and the capsule.

Exopolysaccharide was isolated from culture supernatants by precipitation with ethanol and CTAB, a cationic detergent, a standard protocol described in the literature (4), or by the recently described ultrafiltration method (17). Sugar composition analysis showed Man, Xyl, and GlcA in all of the samples studied, consistent with the proposed structures of cryptococcal PS. Gal was found in small amounts in all of the samples, and it probably originated from the presence of GalXM since we analyzed the complete PS. Based on a previous report determining the molecular ratio of monosaccharides in this PS (22), we calculated the relative amount of GalXM in each of the samples used in this study. The amount of GalXM in the capsular PS fractions was as expected (Table 1), since the galactose-containing PS is one of the components of the cryptococcal capsule. The presence of small amounts of GalXM in exopolysaccharide fractions may indicate that these PSs can form mixed aggregates. To investigate this possibility, we added purified GalXM to PS at a PS-GalXM ratio of 80:20 (wt/wt) and noted a marked increase in molecular mass, suggesting that GalXM binds to PS or that it promotes its aggregation. Hence, the small amounts of GalXM in PS preparations could reflect coprecipitation heteropolymers, and the generation of purer PS preparations may require the use of GalXM-deficient mutant strains (14). The relatively small amount of GalXM in the four samples indicates that the contribution of this PS to the average measurements presented in this study is small, with the caveat that it may contribute to differences in apparent molecular mass if, indeed, it promotes PS aggregation. However, these results also indicate that assigning specific biological functions to PS preparations should be done cautiously, since GalXM is a powerful immunomodulator (18) and even small amounts of GalXM in PS preparations may produce confounding results.

Even considering the presence of GalXM in the PS fractions, the percent composition of each sugar differed between samples. In all of the samples, the mole percentage of Man was higher than the mole percentage of Xyl. This result is supported by a previous study (4) which showed only the presence of PS motif M1 (Man_3-GlcA-Xyl) in the PS isolated from strain 24067. CTAB precipitation and filtration may yield qualitatively different PS preparations than capsular PS from dif-

TABLE 5. Effect of GalXM on *dn/dc*, M_w, *Rg*, M_w/Rg, A_2,and rigidity for 5 and 3 sugars of F and R-F-PS fractions

PS sample with 80:20 (wt/wt) GalXM	*dn/dc* (620 nm)	M_w (10^6 g/mol)[a]	*Rg* (nm)[a]	M_w/Rg (10^3)	A_2 (10^3 cm^{3}mol/g^2)[a]	Rigidity	
						5 sugars	3 sugars
F-PS	0.1452	26 ± 1.2	207 ± 12	125.6	−0.03 ± 0.9	0.2677	0.4462
R-F-PS	0.1274	41 ± 0.2	109 ± 12	376.1	−0.33 ± 0.49	0.047	0.0784

[a] Values are averages and standard deviations.

TABLE 6. Effect of GalXM on charge, mobility, and frequency shift values of F- and R-F-PS fractions calculated by Zeta potential analyzer

PS sample	Zeta potential (mV)	Mobility [(μm/s)/(V/cm)]	Frequency shift (Hz)
F-PS	−42.12 ± 0.14[a]	−2.82 ± 0.12	−22.32 ± 0.22
R-F-PS	−33.92 ± 0.21	−2.65 ± 0.19	−20.46 ± 0.12

[a] Values are averages and standard deviations.

ferences in sugar concentration and PS molecular mass (see below). For the PS isolated from the *C. neoformans* capsule by gamma radiation and DMSO extraction, the molar ratio of monosaccharides was similar but differed from that of the capsular PS. We measured large amounts of glucose in the two fractions of PS isolated from cells, namely, the DMSO-PS and GR-PS fractions. Glucose is not a component of GXM, and the capsule is not thought to contain glucans even though the attachment of GXM to the cell wall is thought to involve GXM-glucan interactions (19). The finding of glucose in capsular PS preparations implies either the presence of glucan moieties in the capsule or the release of glucans from the cell wall by DMSO and gamma radiation. Evidence for non-PS components in the capsule is provided by the observation that it contains chitin-like components (20). Nevertheless, our finding of a significant amount of glucose-containing PS in DMSO-extracted material from acapsular cap67 cells strongly suggests that the glucose in DMSO-PS is derived from PS of cell wall or cell body origin. Glycosyl analysis of DMSO-PS material fractionated by size exclusion chromatography revealed that the larger molecules with higher molecular weights that contained mannose and galactose, but no glucose, are almost certainly PS from the capsule and not glucans from the cell wall. In contrast, glucose was found in the lower-molecular-weight fractions, where galactose was also found. On the basis of these results, we identify the large fibrils found in the DMSO-PS as GXM combined with GalXM.

The CTAB method widely used for GXM purification is plagued by the difficulty in removing this detergent from the PS preparation. The usual method of removing CTAB from GXM is prolonged dialysis against NaCl and water, but there is no good way to establish whether all of the cationic detergent is removed by dialysis. The finding that CTAB-purified PS had a mass that was about 10-fold greater than that of F-PS implies that structural changes were induced by detergent binding, possibly in the form of PS aggregation. In this regard, CTAB appears to promote the aggregation of PS molecules and these may remain in an aggregated state even after the CTAB is presumably removed. CD spectral analysis revealed larger molar ellipticity signals in the far-UV region for CTAB-PS than F-PS, indicating that CTAB purification induced a conformational change in PS.

Analysis of PS fractions by several physical techniques revealed additional differences in the fractions studied. Measurements of molecular weight, radius of gyration, mass density, second virial coefficient, rigidity, viscosity, zeta potential, mobility, and frequency shift each indicated that significant differences for PS were recovered by the different methods described here. In fact, our results demonstrate that radiation also has an impact on the properties of PS, since clear differences in its physical chemical features were induced after treatment with gamma radiation. Gamma radiation generates highly reactive OH and H radicals through the radiolysis of water, which may promote the removal of parts of the PS capsule by a chemical reaction that breaks the polymer into smaller fragments and/or disrupts noncovalent interactions holding the capsule together (2). Smaller PS fragments generated via free-radical attack may also exist as free radicals for a period of time sufficient to react with other PS molecules,

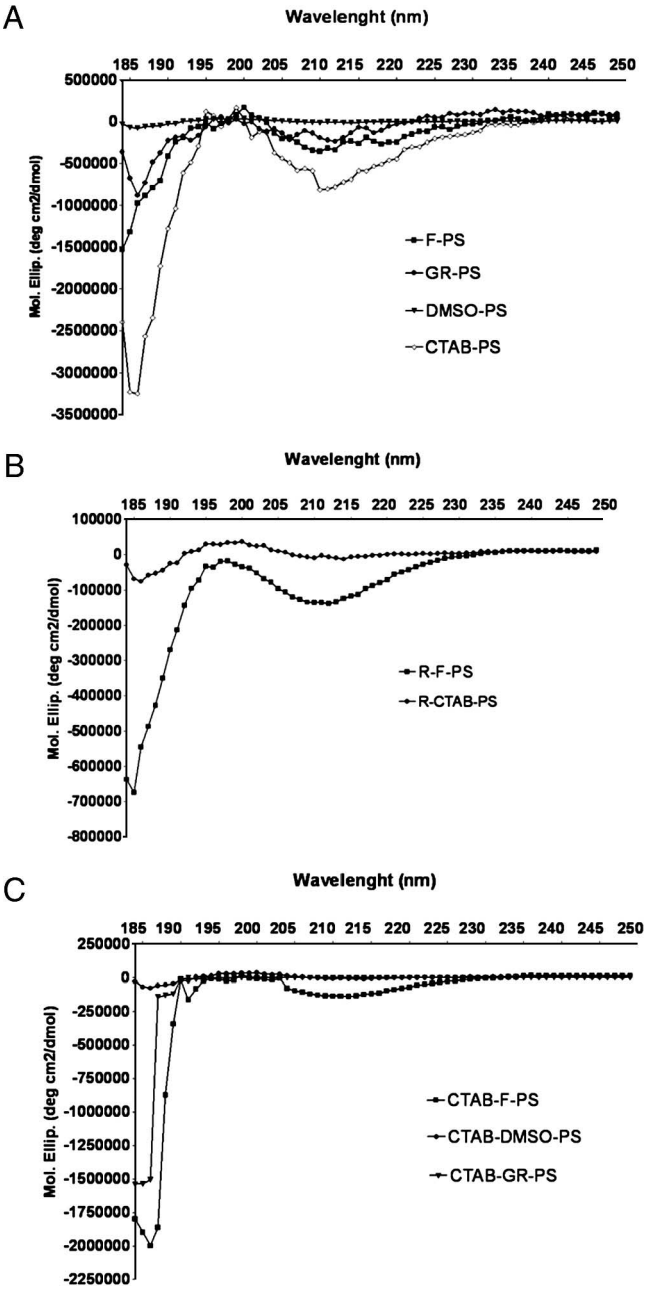

FIG. 3. CD spectra of PS fraction before (A) and after (B) radiation and after CTAB treatment (C). The *x* axis represents the wavelength scanned. The *y* axis shows molar ellipticity (Mol. Ellip.) values expressed in deg cm^2/dmol.

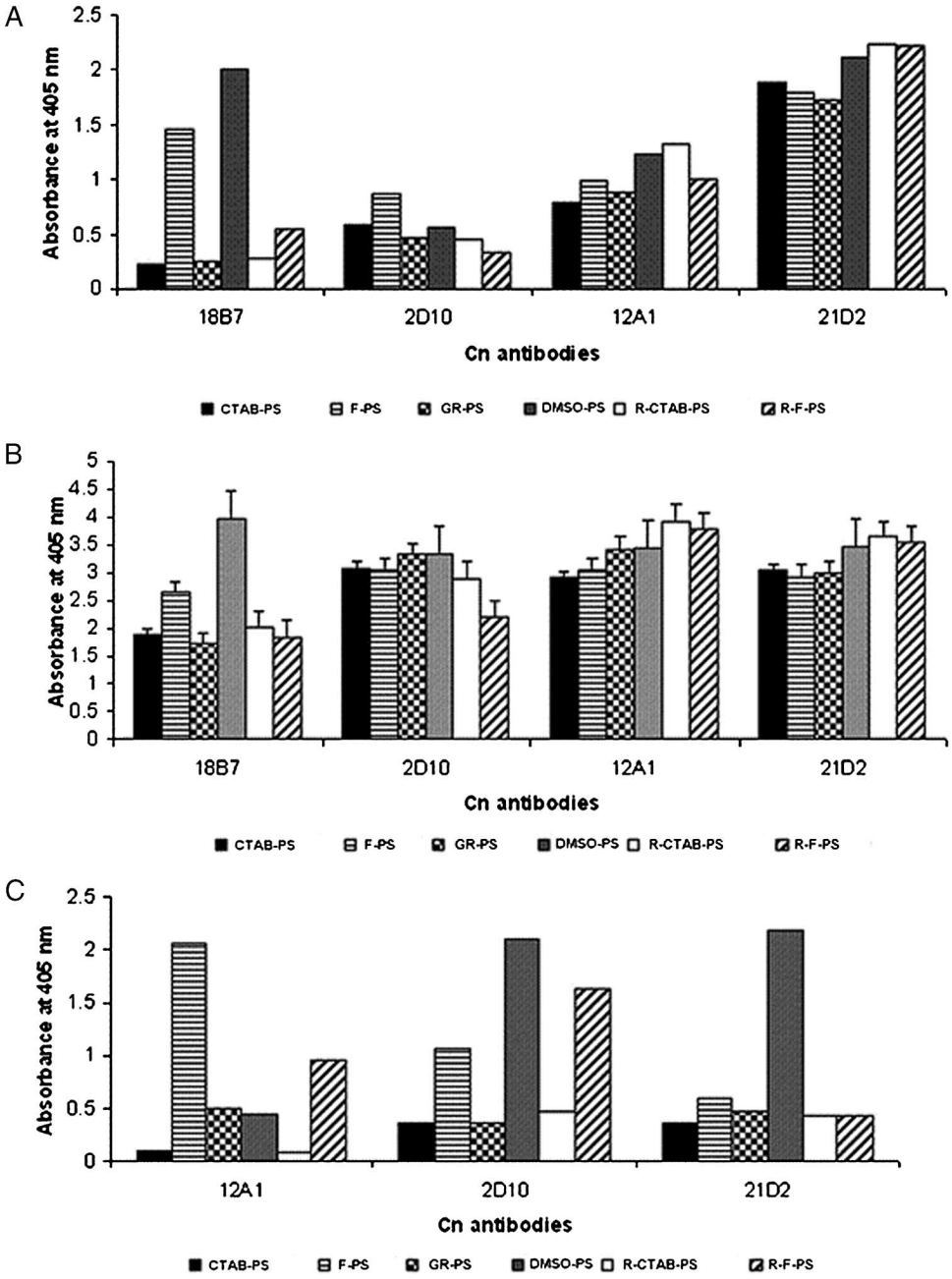

FIG. 4. Binding of MAbs to PS fractions in polystyrene plates (A), dot blot analysis (B), and capture ELISA (C). The *x* axis represents different MAbs. The *y* axis represents absorbance at 405 nm. Cn, *Cryptococcus neoformans*.

resulting in a cross-linking effect (2). Taken together, these results indicate that different biological effects of PS could be expected with different PS preparations. In addition, different physical chemical properties could result, among other effects, in different profiles of receptor and antibody binding. To address this question, we compared the reactivities of different MAbs to PS against the PS preparations analyzed in this study by three different serological methods. Irrespective of the method used, significant differences were noted in the reactivity of PS, indicating that the structural differences inferred from the various physical and chemical analyses translated into antigenic differences.

The finding of antigenic differences between CTAB- and F-PS has important implications for vaccine design. In this regard, it is noteworthy that two PS vaccines have been studied, each eliciting very different types of antibody responses. An earlier vaccine made from exopolysaccharide isolated from culture supernatants (by alcohol precipitation) was not protective despite eliciting high antibody titers. In contrast, a conjugate vaccine made with CTAB-purified PS was protective in

mice (6). Given our findings that F- and CTAB-PS have significant physical, chemical, and antigenic differences, it is intriguing to consider that CTAB purification may alter the PS to enhance its potential usefulness as a vaccine antigen. The different profiles of antibody binding to each of the samples confirmed that the particular structural features may have an impact on PS biological properties. Although the MAbs used in this study were generated from mice immunized with CTAB-PS (16), they bound more intensively to F-PS. This observation may be explained by differential epitope accessibility in the filtered fraction. Radiation of PS increased antibody binding, supporting the hypothesis that epitope exposure in PS may vary according to parameters such as the rigidity, electronegativity, and diameter of the molecule. These results could be related to the well-known differences observed in the pattern of antibody binding to *C. neoformans* cells (15, 16).

In summary, our results reveal significant differences between capsular PS and exopolysaccharide. The physical, chemical, and antigenic properties of PS varied with the purification method used, and this observation raises major questions about the relationship between the structures of native and purified PS and the relevant biological and immunomodulatory activities in vivo.

ACKNOWLEDGMENTS

Funding for this project was provided by NIH awards AI033774, 5R01HL059842, and 2R37AI033142. Carbohydrate and NMR analyses were performed at the Complex Carbohydrate Research Center, University of Georgia (Atlanta), which is supported in part by the Department of Energy-funded (DE-FG-9-93ER-20097) Center for Plant and Microbial Complex Carbohydrates.

We thank Marcio L. Rodrigues, Allan J. Guimaraes, Johanna Rivera, and Joshua Nosanchuk for discussions and assistance with various aspects of this work.

REFERENCES

1. **Bacon, B. E., R. Cherniak, K. J. Kwon-Chung, and E. S. Jacobson.** 1996. Structure of the O-deacetylated glucuronoxylomannan from Cryptococcus neoformans Cap70 as determined by 2D NMR spectroscopy. Carbohydr. Res. **283:**95–110.
2. **Bryan, R. A., O. Zaragoza, T. Zhang, G. Ortiz, A. Casadevall, and E. Dadachova.** 2005. Radiological studies reveal radial differences in the architecture of the polysaccharide capsule of *Cryptococcus neoformans*. Eukaryot. Cell **4:**465–475.
3. **Casadevall, A., J. Mukherjee, and M. D. Scharff.** 1992. Monoclonal antibody based ELISAs for cryptococcal polysaccharide. J. Immunol. Methods **154:** 27–35.
4. **Cherniak, R., H. Valafar, L. C. Morris, and F. Valafar.** 1998. Cryptococcus neoformans chemotyping by quantitative analysis of ^{1}H nuclear magnetic resonance spectra of glucuronoxylomannans with a computer-simulated artificial neural network. Clin. Diagn. Lab. Immunol. **5:**146–159.
5. **Datta, K., and L. A. Pirofski.** 2006. Towards a vaccine for Cryptococcus neoformans: principles and caveats. FEMS Yeast Res. **6:**525–536.
6. **Devi, S. J.** 1996. Preclinical efficacy of a glucuronoxylomannan-tetanus toxoid conjugate vaccine of Cryptococcus neoformans in a murine model. Vaccine **14:**841–844.
7. **Duro, R. M., D. Netski, P. Thorkildson, and T. R. Kozel.** 2003. Contribution of epitope specificity to the binding of monoclonal antibodies to the capsule of Cryptococcus neoformans and the soluble form of its major polysaccharide, glucuronoxylomannan. Clin. Diagn. Lab. Immunol. **10:**252–258.
8. **Gates, M. A., P. Thorkildson, and T. R. Kozel.** 2004. Molecular architecture of the Cryptococcus neoformans capsule. Mol. Microbiol. **52:**13–24.
9. **James, P. G., R. Cherniak, R. G. Jones, C. A. Stortz, and E. Reiss.** 1990. Cell-wall glucans of Cryptococcus neoformans Cap 67. Carbohydr. Res. **198:**23–38.
10. **Maxson, M. E., E. Dadachova, A. Casadevall, and O. Zaragoza.** 2007. Radial mass density, charge, and epitope distribution in the *Cryptococcus neoformans* capsule. Eukaryot. Cell **6:**95–109.
11. **McFadden, D., O. Zaragoza, and A. Casadevall.** 2006. The capsular dynamics of Cryptococcus neoformans. Trends Microbiol. **14:**497–505.
12. **McFadden, D. C., M. De Jesus, and A. Casadevall.** 2006. The physical properties of the capsular polysaccharides from Cryptococcus neoformans suggest features for capsule construction. J. Biol. Chem. **281:**1868–1875.
13. **Monari, C., F. Bistoni, and A. Vecchiarelli.** 2006. Glucuronoxylomannan exhibits potent immunosuppressive properties. FEMS Yeast Res. **6:**537–542.
14. **Moyrand, F., T. Fontaine, and G. Janbon.** 2007. Systematic capsule gene disruption reveals the central role of galactose metabolism on Cryptococcus neoformans virulence. Mol. Microbiol. **64:**771–781.
15. **Nakouzi, A., and A. Casadevall.** 2003. The function of conserved amino acids in or near the complementarity determining regions for related antibodies to Cryptococcus neoformans glucuronoxylomannan. Mol. Immunol. **40:**351–361.
16. **Nakouzi, A., P. Valadon, J. Nosanchuk, N. Green, and A. Casadevall.** 2001. Molecular basis for immunoglobulin M specificity to epitopes in *Cryptococcus neoformans* polysaccharide that elicit protective and nonprotective antibodies. Infect. Immun. **69:**3398–3409.
17. **Nimrichter, L., S. Frases, L. P. Cinelli, N. B. Viana, A. Nakouzi, L. R. Travassos, A. Casadevall, and M. L. Rodrigues.** 2007. Self-aggregation of *Cryptococcus neoformans* capsular glucuronoxylomannan is dependent on divalent cations. Eukaryot. Cell **6:**1400–1410.
18. **Pericolini, E., E. Cenci, C. Monari, M. De Jesus, F. Bistoni, A. Casadevall, and A. Vecchiarelli.** 2006. Cryptococcus neoformans capsular polysaccharide component galactoxylomannan induces apoptosis of human T-cells through activation of caspase-8. Cell. Microbiol. **8:**267–275.
19. **Reese, A. J., and T. L. Doering.** 2003. Cell wall α-1,3-glucan is required to anchor the Cryptococcus neoformans capsule. Mol. Microbiol. **50:**1401–1409.
20. **Rodrigues, M. L., M. Alvarez, F. L. Fonseca, and A. Casadevall.** 26 November 2007, posting date. Binding of the wheat germ lectin to *Cryptococcus neoformans* suggests an association of chitin-like structures with yeast budding and capsular glucuronoxylomannan. Eukaryot. Cell doi:10.1128/EC.00307–07.
21. **Sist, P., P. Cescutti, S. Skerlavaj, R. Urbani, J. H. Leitao, I. Sa-Correia, and R. Rizzo.** 2003. Macromolecular and solution properties of cepacian: the exopolysaccharide produced by a strain of *Burkholderia cepacia* isolated from a cystic fibrosis patient. Carbohydr. Res. **338:**1861–1867.
22. **Vaishnav, V. V., B. E. Bacon, M. O'Neill, and R. Cherniak.** 1998. Structural characterization of the galactoxylomannan of Cryptococcus neoformans Cap67. Carbohydr. Res. **306:**315–330.